

Investigation of Bulk Metallic Glass Tooling Lifetime for Microinjection Molding

Ahmed Almalki^{1,3}, Ali Rajhi², Hussam Noor^{1,3}, Animesh Kundu¹ and John Coulter¹

¹Manufacturing Science Laboratory, Lehigh University, Bethlehem, PA, USA, jc0i@lehigh.edu

²King Khalid University, Abha, Saudi Arabia, arajhi@kku.edu.sa

³Taibah University, Madinah, Saudi Arabia, aamalki@taibah.edu.sa

ABSTRACT

The lifetime of a commercially available zirconium based bulk metallic glass (BMG) for microinjection molding (μ IM) was investigated in this research. The primary objective was to understand the effect of the molding conditions on the BMG tooling. The composition of the Zr-based BMG alloy was $Zr_{67}Cu_{10.6}Ni_{9.8}Ti_{8.8}Be_{3.8}$. A focused ion beam (FIB) milling process was utilized to fabricate the microfeatures. The microfeatures were circular cross-section, 5 μ m in diameter with diameter to depth aspect ratio of 1, and 10 μ m edge-to-edge. The optimal molding processing parameters were initially obtained using MoldFlow simulation. The durability of the BMG mold was investigated by molding parts of thermoplastic polyurethane (TPU) material. The BMG insert was successfully utilized 1000 cycles of μ IM. It was mechanically stable during these experiments. Even after potential crystallization, no sign of any crack initiation was observed in any part of the BMG mold insert. The replication quality degraded with increasing molding cycles. However, the replication quality improved when the cavities were cleaned on heating to an elevated temperature after 750 cycles of injection molding.

Keywords: microinjection molding, bulk metallic glass, MoldFlow, tooling lifetime

1 INTRODUCTION

Microinjection molding of polymeric biomedical devices with micro and sub-micron features is currently affected by the limited tooling life. Large-scale manufacturing requires robust, durable, wear resistant tooling with prolonged lifetime. Also, a tooling needs to preserve features geometry for tens of thousands of molding cycles. Additionally, the tooling components should be manufactured with the required feature size, aspect ratio and surface finish in mind and provide an optimal cost/performance ratio.

Unlike steel and other metals, bulk metallic glass (BMG) superior mechanical properties and its ability to incorporate such features encourages its use for tooling insert in microinjection molding [1]. Specifically, Zr-based BMG has been used extensively for tooling of microinjection molding [2-4]. It was reported that a Zr-BMG tooling endured 20,000 cycles of μ IM with minimal degradation of the replicability [5]. Furthermore, the focused ion beam (FIB) milling process has been utilized for milling features

at the nano and microscale. Although this technique provides high quality surface finish, the low milling rate is the main shortcoming of this technique [6].

In this research, tapered circular cavities were ion-milled on a commercially available Zr-based BMG insert. FEI Scios dual-beam focused ion beam was utilized. Microfeatures have a diameter of 5 μ m, a depth of 5 μ m, and 10 μ m edge-to-edge distance. The durability of the BMG mold was investigated by molding parts of thermoplastic polyurethane (TPU) material. Samples were used to evaluate replication quality and success rate of replicated features.

2 EXPERIMENTAL

2.1 BMG-based Tooling Fabrication

To fabricate the microfeatures onto the BMG mold insert, FIB direct milling process was utilized. A commercially available Vitreloy-1b (Zr-based) BMG alloy was obtained for this research. Table 1 shows its composition and properties. The 6-mm thick BMG plate was diced into blocks of 12 \times 12 mm then it was cleaned from debris.

Composition (wt%)	$Zr_{67}Cu_{10.6}Ni_{9.8}Ti_{8.8}Be_{3.8}$
Yield Strength	1800 MPa
Elastic Modulus	95 GPa
Fracture Toughness	55 MPa.m ^{1/2}
Density	6.0 g/cc
Glass Transition Temperature	352 °C
Crystallization Temperature	466 °C
Melt Temperature	644 °C

Table 1: Vitreloy-1b Zr-BMG alloy properties

The ion beam tends to have a Gaussian profile that intensifies at the middle. This property produces the tapered shape of the milled cavities. It was targeted for optimal demolding of the microfeatures [7].

Figure 1 illustrates the taper-shaped cross-section of the microcavity. A set of FIB milling experiments were performed to determine the optimal FIB milling parameters. It was observed that an ion beam current of 50 nA at 30 KeV Ga⁺ with a dwell time 1 μ s were the most efficient conditions for the microfeatures fabrication on the BMG mold insert.

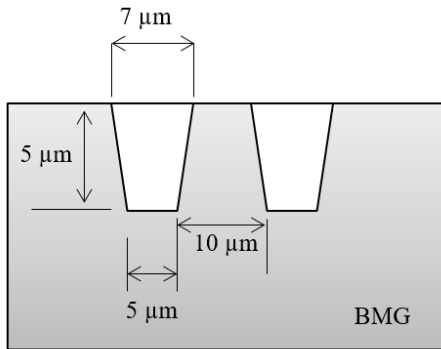


Figure 1: Schematic cross-sectional view of the tapered-shape microcavity

Multiple arrays of 10×10 microcavities were milled covering a total area of $\sim 0.26 \text{ mm}^2$ at the middle of the BMG insert. Figure 2 shows the fabricated BMG mold insert. The total number of microcavities in the insert was 1200. After the completion of the milling, the insert was installed into the mold assembly using Epoxy resin for molding experiments.

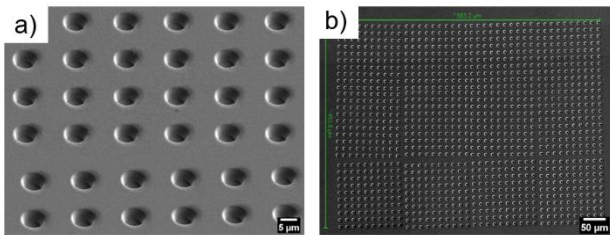


Figure 2: The fabricated BMG mold insert a) Tilted view and b) top view

The BMG insert was used to mold TPU parts. The optimal processing parameters for μIM was obtained from MoldFlow simulations. Periodically, the BMG insert was inspected using scanning electron microscopy (SEM) to observe changes through molding cycles. Also, samples were used to evaluate replication quality and success rate of replicated features.

2.2 MoldFlow Simulations

A CAD model representing the molded part with microfeatures was developed using SolidWorks. The model was then imported into MoldFlow software. Micropillars were modeled in a 15×15 array formation instead of a 40×30 array that was utilized in the actual experiments to reduce the computational time. The features had a diameter of $5 \mu\text{m}$, a height of $5 \mu\text{m}$, and an edge-to-edge distance of $10 \mu\text{m}$. Molding window analysis and dual domain meshing were utilized to obtain recommended processing parameters before performing 3D simulations.

The meshing of the molded part was optimized by controlling the meshing density. A multi-scale meshing strategy was utilized for the sprue and the microfeatures as illustrated in Figure 3. The edge length for the sprue was set to 0.25 mm , while the edge length for the microfeatures was set to 0.0025 mm . The resultant mesh has more than 330,000 tetrahedral elements.

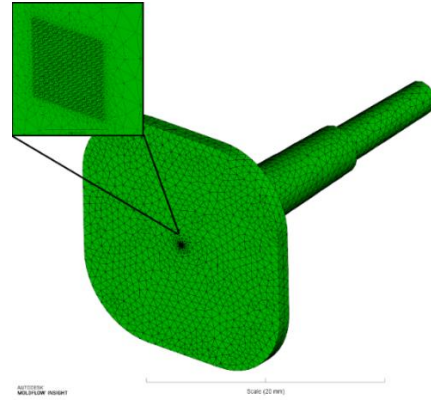


Figure 3: Multi-scale meshing of the molded part

Multiple simulation case studies were performed for the filling and packing analysis to achieve optimal processing parameters. Table 2 lists the molding parameters used for molding of TPU (Texin985). The simulations indicated that it would require 0.24 seconds for the mold to be completely filled under the optimal conditions as shown in Figure 4. It would require ~ 0.12 seconds to fill the microcavities.

Fill time [Seconds]	0.24
Melt Temperature [$^{\circ}\text{C}$]	205
Mold Temperature [$^{\circ}\text{C}$]	50
Injection Pressure [MPa]	40
Packing Pressure [MPa]	80
Cooling Time [Seconds]	125

Table 2: Optimal molding parameters for TPU (Texin 985)

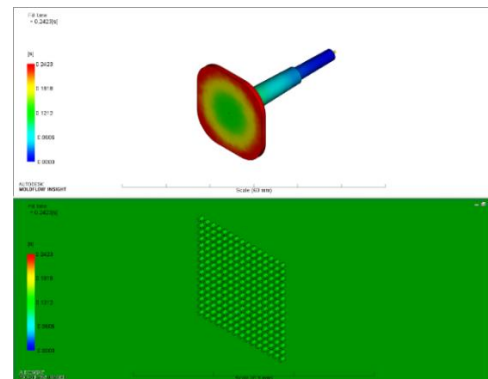


Figure 4: MoldFlow simulations results of the cavity filling time

2.3 Microinjection Molding

Experimental validations were performed using a 3-ton Nissei-AU3E microinjection molding machine. TPU (Texin 985) material was used to mold samples with desired micropillars. After acquiring optimal processing parameters from MoldFlow simulation software, several short shots trials were performed for calibration purposes. A total number of 1000 of molding cycles were performed utilizing the BMG mold insert. Experimental design was set to inspect the BMG insert and the corresponding samples periodically. Samples were inspected utilizing SEM. The SEM images were processed using ImageJ software to assess the features replication efficacy.

3 RESULTS AND DISCUSSION

3.1 Effect of Mold Assembly Heating

The BMG mold insert surface morphology changed dramatically on heating. A series of wrinkles appeared on the originally flat surface (Figure 5). The wrinkles extended to the edges of the microcavities. As a result, the edges of the microcavities were deformed. The walls and the bottom of cavities were unaffected. It was hypothesized that the mold insert has crystallized. The crystallization temperature for Vitrelloy-1b has been reported to be 446 °C.

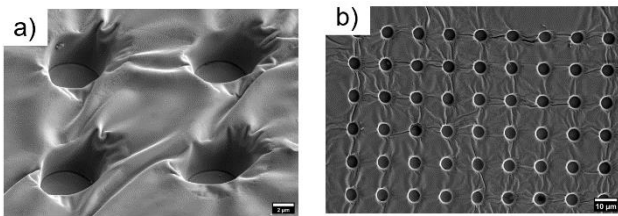


Figure 5: The BMG mold after 750 cycles a) Tilted view and b) top view

In addition, the residual polymer that was left from the molding experiments in microcavities were removed because of this heating. The cavity geometry, the BMG surface quality, and the cleanliness of the cavity changed after the heating; thus, results of the molding experiments were compared in two batches: samples that were fabricated up to 750 cycles and samples that were fabricated from 751 up to 1000 cycles.

The molding insert was mechanically stable during these experiments. The wrinkles on the surface after crystallization provided additional stress concentrating regions that could have led to mechanical failure of the insert in the subsequent molding experiments. However, there was no sign of crack initiation in any part of the BMG mold insert even when it was crystallized.

3.2 Quantification of Replication Efficacy

The height and the diameter of the molded micropillars were utilized to determine the efficacy of the molding process. The height of the microfeatures was considered to be indicative of the replication quality. A term replication quotient (RQ), defined as the micropillar height divided by the cavity depth, was utilized for quantification of the replication quality. For each sample, a total of random 220 micropillar heights were measured. It was determined that this would sufficiently represent the entire sample.

The diameter of the molded microfeatures were considered to be indicative of the successful molding in this study. The threshold diameter was set at 90% of the intended diameter. Since the microcavities had a base diameter of 5 μm , the fraction of the molded pillars with microfeature diameter more than 4.5 μm was utilized to measure the “success rate”. Figure 6 shows the sequence for the threshold process of the sample #100.

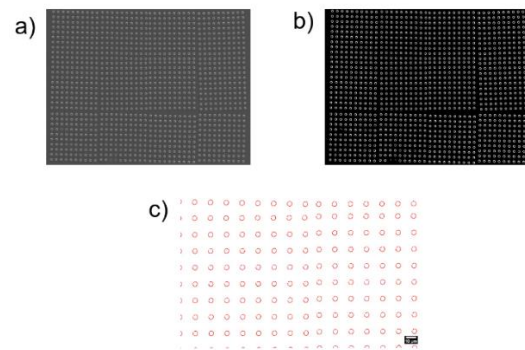


Figure 6: a) Raw SEM image of molded sample #100. b) Threshold binary image. c) Magnified image of successful features

3.3 Pre-crystallization Molding (<750 Cycles)

Figure 7 presents the RQ of the samples fabricated during the first 750 molding cycles. The mean value and the range of the distribution is presented in the figure. It was observed that the mean RQ decreased with molding cycles from 0.9 at 100 cycles to 0.7 at 600 cycles. The distribution of the pillar heights was also wider for the higher molding cycle numbers. This was attributed to the adherence of the polymers to the base of the microcavities. A representative SEM micrograph of such adherence is shown in Figure 8. The temperature profile of the die assembly needs to be more carefully controlled to avoid such a behavior. A suitable cleaning of the mold insert after the fabrication might be helpful as well. Alternatively, an anti-stiction coating could aid in reducing the adhesion between polymers and the mold surfaces.

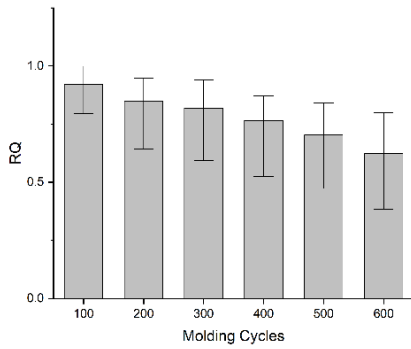


Figure 7: RQ for <750 molding cycles

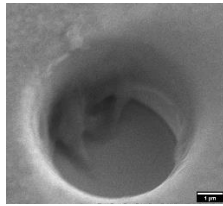


Figure 8: Residues of the polymer within the microcavity after 250 molding cycles

Figure 9 shows the success rate through molding cycles. It can be observed that more unsuccessful features occurred at higher number of molding cycles. As a result, features tend to be replicated with diameters less than 4.5 μm as the residues inside microcavities stripped micropillars tips.

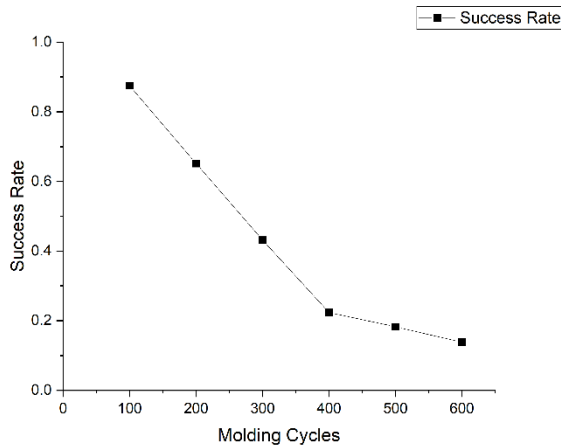


Figure 9: Success rate through molding cycles

3.4 Post-crystallization Molding (>750 Cycles)

After the BMG insert crystallization, no sign of mechanical failure occurred to the BMG mold insert during the subsequent μIM for an additional 250 cycles.

RQ through molding cycles after the BMG insert crystallization is presented in Figure 10. Elevated temperatures caused the polymer residues to melt and had a self-cleaning effect. As a result, the RQ increased from 0.7 at cycle #600 up to 0.9 at cycle #750. The RQ decreased progressively from 0.9 at cycles #750 to ~ 0.72 at cycle #1000.

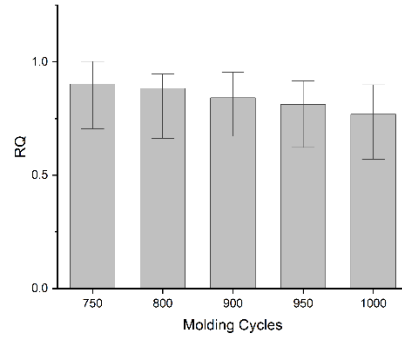


Figure 10: RQ for >750 molding cycles

Additionally, the nanofeatures that occurred on the insert's surface because of the crystallization were replicated perfectly during the post crystallization molding. A representative SEM micrograph is presented in Figure 11.

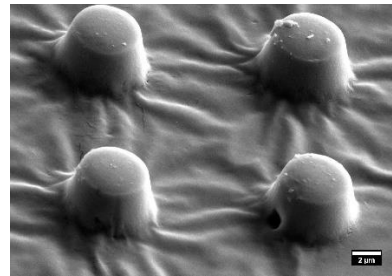


Figure 11: Molded sample # 900 with nanofeatures on the surface

Further investigations are required to determine optimal molding conditions and thermal designs to avoid polymer adhesion. Alternatively, a carefully regulated mold assembly cleaning procedure at elevated temperatures could be developed for cavity cleaning between cycles.

4 CONCLUSION

A commercially available Zr-based BMG insert was successfully utilized 1000 cycles of microinjection molding. The molding insert was mechanically stable during these experiments. Even after potential crystallization, no sign of any crack initiation was observed in any part of the BMG mold insert.

The replication quality degraded with increasing molding cycles. The adhesion of the polymer to the bottom of the microcavities were attributed to the degradation of the replication quality. The replication quality improved when the cavities were cleaned on heating to an elevated temperature after 750 cycles of injection molding. Also, nanofeatures that occurred on the insert's surface were replicated perfectly indicating that the BMG mold insert could potentially utilized for nano-scale injection molding.

REFERENCES

- [1] Wang, W., Dong, C. and Shek, C., 2004. Bulk metallic glasses. *Materials Science and Engineering: R: Reports*, 44(2-3), pp.45-89.
- [2] He, P., Li, L., Wang, F., Dambon, O., Klocke, F., Flores, K. and Yi, A., 2014. Bulk metallic glass mold for high volume fabrication of micro optics. *Microsystem Technologies*, 22(3), pp.617-623.
- [3] Kündig, A., Cucinelli, M., Uggowitzer, P. and Dommann, A., 2003. Preparation of high aspect ratio surface microstructures out of a Zr-based bulk metallic glass. *Microelectronic Engineering*, 67-68, pp.405-409.
- [4] Zhang, N., Srivastava, A., Browne, D. and Gilchrist, M., 2016. Performance of nickel and bulk metallic glass as tool inserts for the microinjection molding of polymeric microfluidic devices. *Journal of Materials Processing Technology*, 231, pp.288-300.
- [5] Zhang, N., Chu, J., Byrne, C., Browne, D. and Gilchrist, M., 2012. Replication of micro/nano-scale features by micro injection molding with a bulk metallic glass mold insert. *Journal of Micromechanics and Microengineering*, 22(6), p.065019.
- [6] Browne, D., Stratton, D., Gilchrist, M. and Byrne, C., 2012. Bulk Metallic Glass Multiscale Tooling for Molding of Polymers with Micro to Nano Features: A Review. *Metallurgical and Materials Transactions A*, 44(5), pp.2021-2030.
- [7] Giannuzzi, L. and Stevie, F., 2010. *Introduction to focused ion beams*. New York: Springer.